Pressure Effect on the Inter- and Intramolecular Vibrations of Pyrazine Crystal

Masayoshi Maehara, Hiroshi Kawano, Yoshinori Nibu, Hiroko Shimada,* and Ryoichi Shimada†

Department of Chemistry, Faculty of Science, Fukuoka University, Nanakuma, Jonan-ku, Fukuoka 814-80

†Department of General Education, Fukuoka Institute of Technology, Wajiro-Higashi, Higashi-ku, Fukuoka 811-02

(Received July 14, 1994)

The effect of pressure on the Raman active inter- and intramolecular vibrations of the pyrazine crystal was studied under hydrostatic pressure up to 5 GPa. The frequency shift of the intermolecular vibrations and the discontinuous variation of the bandwidth of the ν_2 and ν_1 intramolecular vibrations induced by pressure at constant temperature indicate that the pyrazine crystal undergoes phase transition (change of the molecular orientation in the crystal) under about 1 GPa. The pressure-induced frequency shift of the intramolecular vibrations was calculated using an intermolecular potential of the atom–atom type. The calculation also suggests the occurrence of the phase transition of the crystal.

Thiéry and Léger,[1] Ellenson and Nicol,[2] Adams and Appleby,[3] and Cansell et al.[4] studied the Raman spectrum of the benzene crystal under high pressure and found that the phase transitions of the crystal take place under 1.4, 4, 11, and 24 GPa through observations of the abrupt change of the spectral structure, the shift of the vibrational frequency, and the variation of the bandwidth of the Raman band induced by pressure. Recently we observed the pressure effect on the inter- and intramolecular vibrations of the 1,2,4,5-tetrachloro- and hexachlorobenzene crystals and found the splitting of the band due to the degenerate intramolecular vibrations as well as the phase transition.[5,6]

A number of theoretical studies were made on the frequency shift of the intramolecular vibrations induced by the intermolecular force.[7—10] Very recently we calculated the pressure-induced frequency shift of the intramolecular vibrations of the benzene, hexachloro, and 1,2,4,5-tetrachlorobenzene crystals including the first-order differential of the intermolecular potential, which was generally ignored in the calculation of the pressure-induced frequency shift, and showed that the first-order differential term could be reasonably neglected when the potential is well approximated.[11,12]

A number of works were made on the intramolecular vibrations of pyrazine through observations of the Raman and infrared,[13—16] phosphorescence,[17,18] and fluorescence spectra.[19—21] The intermolecular vibrations of the pyrazine crystal were studied by many workers.[22—24] Sbrana et al.[15] and Schettino et al.[25] found that the pyrazine crystal undergoes the phase transition at 29 °C by observing the temperature effect on the structures of the infrared and Raman spectra due to the intramolecular vibrations and by measuring the differential scanning calorimetry of the pyrazine crystal.

In this work, the effect of pressure on the Raman active inter- and intramolecular vibrations of the pyrazine crystal is observed and the phase transition of the crystal and the pressure-induced frequency shift of the intramolecular vibrations are discussed.

Experimental

Material. [$^2H_4$]Pyrazine was synthesized by the exchange reaction of [$^1H_4$]Pyrazine obtained from Tokyo Kasei Co. with D_2O using palladium asbestos as a catalyst.[26] The samples were purified by repeated vacuum distillations.

Optical Measurement. The Raman active inter- and intramolecular vibrations were measured with a JEOL 400T laser Raman spectrophotometer under various pressures from 1 atm (1×10^{-4} GPa) to 5 GPa at 297 K by the backscattering observation method. The 514.5, 488.0, and 476.5 nm beams from an Ar^+ ion laser were used for the excitation. A diamond anvil cell obtained from Toshiba Tungaloy Co. was used for measurement of the Raman spectrum under high pressure. The sample and ruby chips suspended in cedar wood oil were held in a sample hole made in the stainless steel gasket. The pressure inside the sample hole was determined by measuring the wavelength shift of the fluorescence line at 694.2 nm (R_1 line) emitted from ruby chips using the equation proposed by Mao et al.[27] The pressure was confirmed to be hydrostatic by observing the shapes of the R_1 and R_2 (692.7 nm) lines emitted from ruby. Details of the experiment are exactly the same as those described previously.[5]

Calculation of the Pressure-Induced Frequency Shift of the Intramolecular Vibrations

The frequency shift of the intramolecular vibrations induced by the intermolecular interaction with other molecules are given by[7—10]

$$\Delta\tilde{\nu}_{\text{shift}} = \frac{1}{8\pi^2 c^2 \tilde{\nu}_{Q_n}} \sum_i \sum_j \left(\frac{\partial^2 V_{ij}}{\partial r_{ij}^2}\right)\left(\frac{\partial r_{ij}}{\partial Q_n}\right)^2, \quad (1)$$

where Q_n and $\tilde{\nu}_{Q_n}$ are n-th normal coordinate and its unperturbed vibrational frequency, respectively, r_{ij} is the interatomic distance between atoms i and j belonging to different molecules, and V_{ij} is the potential energy of the atom–atom type due to the intermolecular interaction between two molecules. For the potential, V_{ij} expressed by[28,29]

$$2V_{ij} = [-Ar_{ij}^{-6} + B\exp(-Cr_{ij}) + q_i q_j e^2 r_{ij}^{-1}] \quad (2)$$

was used, where A, B, and C are parameters, and q_i and q_j are the electric charges on the atoms i and j, respectively. The values of the parameters were taken from those given by Spackman[27] and the electric charge was evaluated by the CNDO/2 MO calculation. The electric charges on the N, C, and H atoms were calculated to be $-0.146e$, $0.114e$, and $-0.04e$, respectively, where e is 1.6021×10^{-19} C. The three terms in Eq. 2 represent the dispersive, repulsive, and electrostatic energies, respectively. The values of $\partial^2 V_{ij}/\partial r_{ij}^2$ and $\partial r_{ij}/\partial Q_n$ were calculated in the same way as described previously.[5,6]

A normal coordinate calculation was performed through the standard GF matrix method and the F matrix elements for the in-plane and out-of-plane vibrations were evaluated with the potential fields of the modified Urey–Bradley and the valence force fields, respectively.[30] The force constants were taken from the data given previously.[30]

The molecular orientation in the crystal under 1 atm was taken from the data given by With et al.[31] The molecular orientation in the crystal was assumed to keep unchanged under application of pressure and the atom–atom distance between two molecules was evaluated assuming isotropic compressibility. Three assumptions were made for the molecular geometry, that is, the molecular geometry was assumed to keep unchanged (case A), only the C–H bond length was assumed to change from 0.108 nm[31] to 0.105 nm (case B), and from 0.108 nm to 0.100 nm (case C) by varying pressure from 1 atm to 4.5 GPa.

The pressure-induced frequency shift was calculated changing the intermolecular distances and the intermolecular distance was converted into pressure in exactly the same way as that described previously.[5,6] Since the value of compressibility for the pyrazine crystal is not available, the calculation was made using different values of compressibility given for various molecular crystals such as naphthalene and hexamethylbenzene by Vaidya and Kennedy.[32] The calculation led to the similar results for different values of compressibility and therefore, the value of compressibility for the pyrazine crystal was assumed to be the same as that obtained for the naphthalene crystal.[32]

Results and Discussion

Pressure Effect on the Intermolecular Vibrations. Pyrazine crystallizes in the orthorhombic space group *Pmnn* with two molecules in the unit cell.[31] The Raman spectra of the pyrazine crystal in the intermolecular vibrational region observed under various pressures at 297 K are shown in Fig. 1. The four Raman bands observed at 43, 68, 104, and 115 cm^{-1} under 1 atm were assigned to the intermolecular vibrations of b_{1g}, b_{1g}, a_g, and b_{3g} species, respectively.[24] The shortest wavenumber band resolves into two bands of b_{1g} and b_{2g} species in the spectrum observed at 4.2 K.[24] The Raman spectral structure due to the intermolecular vibrations of the [$^2H_4$]pyrazine crystal is almost equal to the spectral structure of the [$^1H_4$]pyrazine crystal. The observed frequencies of the intermolecular vibrations of the [$^1H_4$]- and [$^2H_4$]pyrazine crystals under various pressures are given in Table 1. The pressure dependence of the Raman frequency, which will be called as pressure–frequency curve hereafter, for the [$^1H_4$]- and

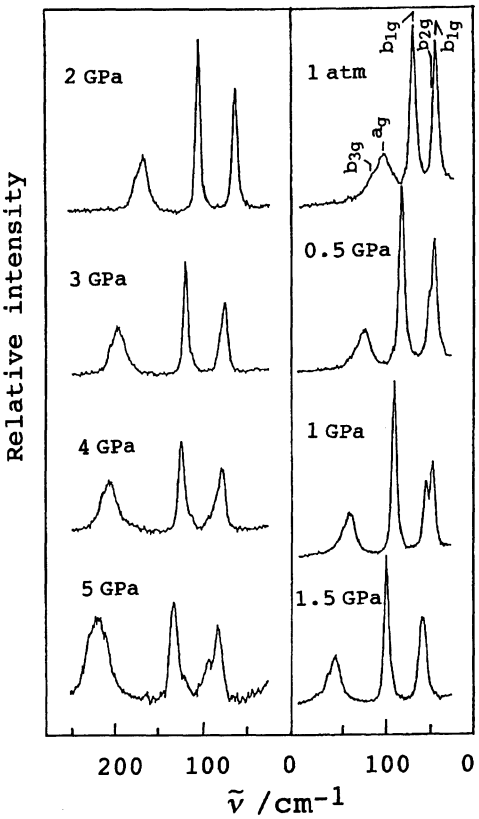

Fig. 1. The Raman spectra of the pyrazine crystal in the intermolecular vibrational region observed under various pressures at 297 K. 1 atm corresponds to 10^{-4} GPa.

Table 1. Observed Frequecy of the Intermolecular Vibrations of the Pyrazine Crystal

	Pressure/GPa									
	1 atm	0.3	0.5	1.0	1.5	2.0	3.0	3.5	4.0	4.5	5.0
$[^1H_4]$[a]		44	45	46	57		74	76	77	79	81
	43					63					
		47	50	53	59		79	83	85	89	93
							111	112	113	115	116
	68	76	81	90	99	103	118	120	124	127	131
	104	116	123	140	156	164	196	200	204	212	213
	115	124	131	151	163	172	202	207	210	220	230
$[^2H_4]$[a]		43	43	45	53	58					
	42						70				
		45	48	53	57	60					
	67	72	80	87	94	99	113				
	93	103	117	135	139	150	175				
	102	111	125	143	147	158	183				

(in cm^{-1} unit)

a) $[^1H_4]$ and $[^2H_4]$ represent $[^1H_4]$- and $[^2H_4]$pyrazines, respectively.

$[^2H_4]$pyrazine crystals is given in Fig. 2. The shortest wavenumber band splits into doublet by applying pressure. The splitting becomes larger up to about 1 GPa with increasing pressure and then becomes smaller up to about 2 GPa. The splitting is hardly detectable under about 2 GPa and then becomes clearly detectable again over pressure from about 2.5 GPa. Another weak band is observed as the shoulder of the second shortest wavenumber bands of b_{1g} species from pressure of about 2 GPa for the $[^1H_4]$pyrazine crystal. These observations suggest that the phase transition takes place in the pyrazine crystal under about 1 GPa.

Pressure Effect on the Intramolecular Vibrations. The Raman bands observed at 601, 700, 758, 943, 978, 1019, 1250, 1521, 1582, 3032, and 3047 cm^{-1} under 1 atm at 297 K were assigned to the intramolecular ν_{6a}, ν_{6b}, ν_4, ν_{10a}, ν_5, ν_1, ν_{9a}, ν_{8b}, ν_{8a}, ν_{7b}, and ν_2 vibrations, respectively.[12—16,19,21] The all Raman bands except for the ν_{6a} and ν_4 bands were clearly resolved under high pressure up to about 5 GPa. The Raman spectra observed under various pressures are shown in Fig. 3. The vibrational frequencies observed in vapor and in crystal under 1 atm and 4.5 GPa are given in Table 2. The calculation of the pressure-induced frequency shift was carried out considering the intermolecular interactions with the eight surrounding molecules for three different molecular geometries described above under pressure up to 4.5 GPa. The calculated results are given in Tables 3 and 4, together with the observed frequency shift.

The frequency shift induced by the change of the phase from vapor to crystal under 1 atm will be discussed first. The vibrational frequency of pyrazine in vapor phase was obtained from the fluorescence spectrum in a supersonic free jet, where the molecule is free from the molecular interaction. Therefore the calculated frequency shift for pressure of 1 atm, $\Delta\nu_{1atm}$, can

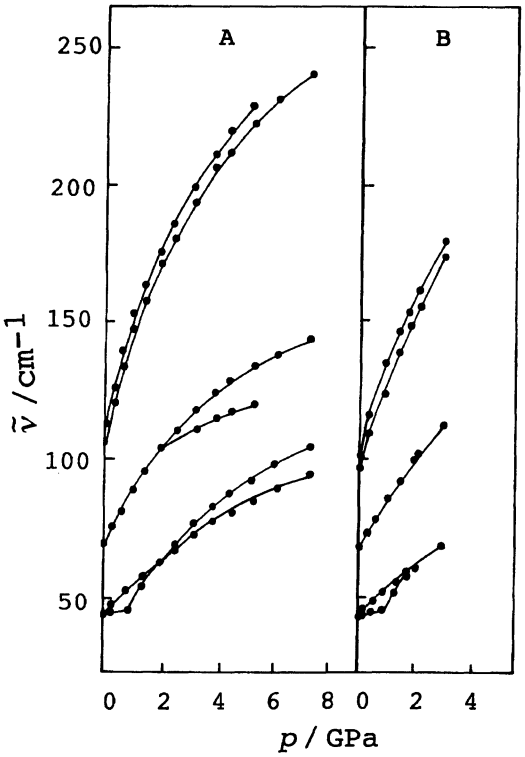

Fig. 2. Pressure effect on the intermolecular vibrational frequencies of the $[^1H_4]$- (A) and $[^2H_4]$pyrazine (B) crystals observed at 297 K.

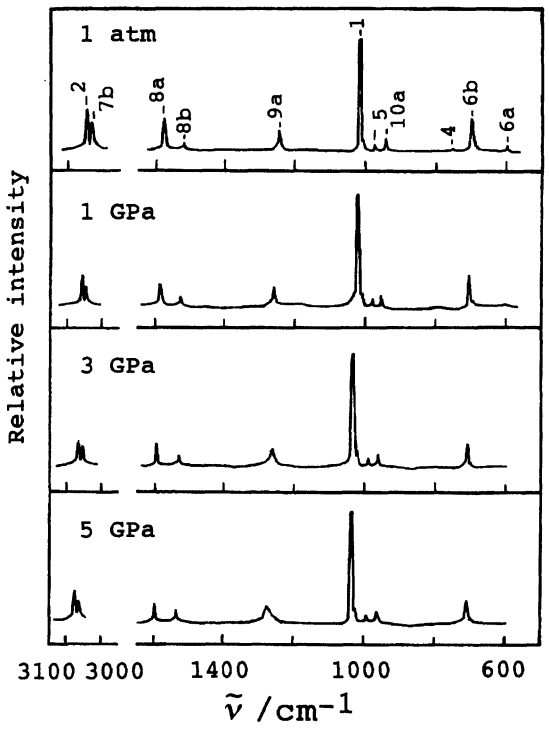

Fig. 3. The Raman spectra of the pyrazine crystal in the intramolecular vibrational region observed under various pressures at 297 K.

Table 2. Observed Frequency of the Intramolecular Vibrations of Pyrazine

Vibrational mode	Vapor[a]	Crystal	
		1 atm	4.5 GPa
	$\tilde{\nu}$/cm^{-1}	$\tilde{\nu}$/cm^{-1}	$\tilde{\nu}$/cm^{-1}
ν_2		3047	3073
ν_{7b}		3032	3056
ν_{8a}	1578	1582	1602
ν_{8b}		1521	1536
ν_{9a}	1231	1250	1284
ν_1	1014	1019	1043
ν_{6a}	596	601	
ν_{6b}	704[b]	700	708
ν_5	965[b]	978	997
ν_{10a}	919	943	973
ν_4	755[b]	758	

a) Taken from Ref. 19. b) Taken from Ref. 21.

Table 3. Calculated and Observed Pressure-Induced Frequency Shifts of the Raman Active Intramolecular Vibrations of the Pyrazine Crystal under 1 atm

Mode	$\Delta\tilde{\nu}_{1atm}$[a]				
	Calcd				Obsd[b]
	Repul	Disp	E.S.	Total	
	$\tilde{\nu}$/cm^{-1}	$\tilde{\nu}$/cm^{-1}	$\tilde{\nu}$/cm^{-1}	$\tilde{\nu}$/cm^{-1}	$\tilde{\nu}$/cm^{-1}
ν_2	25.9	−3.9	0.1	22.1	
ν_{7b}	25.8	−3.9	0.1	22.0	
ν_{8a}	5.3	−1.4	0.0	3.9	4
ν_{8b}	4.9	−1.1	0.0	3.8	
ν_{9a}	23.3	−4.6	0.0	18.7	19
ν_1	13.0	−2.5	0.0	10.5	5
ν_{6a}	15.5	−3.0	0.0	12.5	5
ν_{6b}	14.6	−3.2	0.0	11.4	−4
ν_5	24.1	−6.2	0.0	17.9	22
ν_{10a}	26.0	−6.6	0.1	19.5	24
ν_4	16.8	−4.4	0.1	12.5	3

a) $\Delta\tilde{\nu}_{1atm}=\tilde{\nu}_{1atm}-\tilde{\nu}_{vapor}$. b) See Table 2.

be regarded as the difference of the vibrational frequencies observed in jet and crystal.

The calculated results indicates that (1) the repulsive interaction between the hydrogen and nitrogen atoms belonging to different molecules gives the largest contribution to the frequency shift for the all vibrations and (2) the hydrogen displacement vibrations of the H wagging (ν_{10a} and ν_5), bending (ν_{9a}), and stretching (ν_{7b} and ν_2) modes suffer from the stronger repulsive interaction than the ring vibrations (ν_{8a}, ν_{8b}, ν_1, ν_{6a}, ν_{6b}, and ν_4). The large frequency shifts observed for the ν_{9a}, ν_5, and ν_{10a} vibrations can be well explained by the calculation. The agreement of the observed and calculated frequency shifts is fairly well for the all vibrations except for the ν_{6b} vibration.

Next the pressure-induced frequency shift in crystal under pressure from 1 atm to 4.5 GPa will be discussed. The observed and calculated pressure-induced frequency shifts, $\Delta\tilde{\nu}=\Delta\tilde{\nu}_{pGPa}-\Delta\tilde{\nu}_{1atm}$, are plotted against pressure in Fig. 4. The agreement between the observed and calculated frequency shifts are fairly well for the ring vibrations ν_{8a}, ν_{8b}, and ν_1 (except for the ν_{6b} vibration), while the calculated frequency shifts are much larger than the observed shifts for the H displacement vibrations. The very large discrepancy of the calculated and observed frequency shifts for the H displacement vibrations is considered to be caused by the very large value of the calculated repulsive interaction between adjacent molecules. In the previous works for the pressure-induced frequency shift of the 1,2,4,5-tetrachloro- and hexachlorobenzene crystals it was shown that the agreement between the calculated and observed frequency shifts is fairly well for all vibrations when the

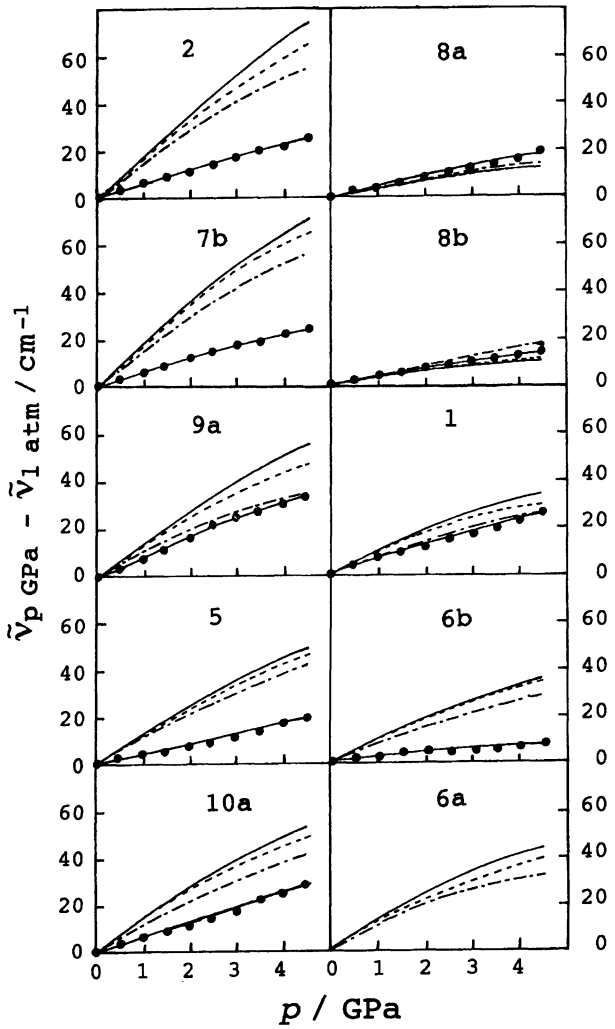

Fig. 4. The observed (•–•–•) and calculated (— for case A, --- for case B, and — — for case C) pressure effects on the vibrational frequencies of the H displacement ν_2, ν_{7b}, ν_{9a}, ν_5, ν_{10a}, and ring ν_{8a}, ν_{8b}, ν_1, ν_{6b}, ν_{6a} vibrational modes of the pyrazine crystal. The difference of the frequency shift, $\Delta\tilde{\nu}=\Delta\tilde{\nu}_{pGPa}-\Delta\tilde{\nu}_{1atm}$, is plotted against pressure.

Table 4. Calculated and Observed Pressure-Induced Frequency Shifts of the Raman Active Intramolecular Vibrations of the Pyrazine Crystal under 4.5 GPa

Mode	$\Delta\tilde{\nu}_{4.5GPa}$[a]				$\Delta\tilde{\nu}_{4.5GPa}-\Delta\tilde{\nu}_{1atm}$	
	Repul	Disp	E.S.	Total	Calcd	Obsd[b]
	$\tilde{\nu}$/cm^{-1}	$\tilde{\nu}$/cm^{-1}	$\tilde{\nu}$/cm^{-1}	$\tilde{\nu}$/cm^{-1}	$\tilde{\nu}$/cm^{-1}	$\tilde{\nu}$/cm^{-1}
ν_2	109.8(89.6)	−14.9(−12.1)	0.3(0.3)	95.2(77.8)	73.1(55.7)	26
ν_{7b}	109.4(89.2)	−14.8(−12.1)	0.3(0.3)	94.9(77.4)	72.9(55.4)	24
ν_{8a}	19.9(23.0)	−3.7(−4.2)	0.0(0.0)	16.2(18.8)	12.3(14.9)	20
ν_{8b}	19.3(28.3)	−3.2(−4.6)	0.0(0.0)	16.1(23.7)	12.3(19.9)	15
ν_{9a}	88.7(64.2)	−14.0(−10.5)	0.0(0.0)	74.7(53.7)	56.0(35.0)	34
ν_1	53.4(41.8)	−8.2(−6.6)	0.0(0.0)	45.2(35.2)	34.7(24.7)	24
ν_{6a}	66.7(53.7)	−10.1(−8.3)	0.0(0.0)	56.6(45.4)	44.1(32.9)	
ν_{6b}	58.0(50.6)	−9.6(−8.6)	0.0(0.0)	48.4(42.0)	37.0(30.6)	8
ν_5	83.6(73.3)	−15.2(−13.8)	0.3(0.2)	68.7(59.7)	50.8(41.8)	19
ν_{10a}	90.8(75.1)	−16.5(−14.1)	0.1(0.2)	74.6(61.2)	55.1(41.7)	30
ν_4	56.6(44.7)	−10.6(−8.9)	0.1(0.1)	46.1(35.9)	33.6(23.4)	

a) $\Delta\tilde{\nu}_{4.5GPa}=\tilde{\nu}_{4.5GPa}-\tilde{\nu}_{vapor}$. b) See Table 2. c) Values inside the parentheses were calculated for the molecular geometry of case C and the values outside the parentheses for the geometry of case A (see text).

phase transition does not take place, whereas the agreement becomes very poor for the chlorine displacement vibrations, which suffer from the strong repulsive interaction, when the phase transition takes place.[5,6]

These facts suggest that the compression increases the intermolecular interaction through strengthening the repulsive forces and the strain of the crystal triggers the phase transition under certain pressure to release from the repulsive forces. As can be seen from Table 4 and Fig. 4, the shortening of the C–H bond distance, which might be induced by applying pressure, causes a slight decrease of the calculated repulsive interaction and as the result the discrepancy of the calculated and observed frequency shifts for the H displacement vibrations is improved slightly. But only the shortening of the C–H bond distance is not sufficiently enough to explain the large discrepancy. This fact suggests that the change of the molecular orientation in the crystal must be taken into account in the calculation of the pressure-induced frequency shift in order to explain the observed frequency shift.

Cansell et al.[31] studied the phase transition of the benzene crystal and showed that unambiguous detection of phase transition is not easy by measuring the pressure–frequency curve of the intramolecular vibrations, while the plot of the bandwidth against pressure at constant temperature, which will be called as the pressure–bandwidth curve hereafter, shows drastic change of the slope by the phase transition. The pressure–bandwidth curves for the ν_1 and ν_2 vibrations of the [$^1H_4$]pyrazine crystal observed at 297 K are given in Fig. 5, where the discontinuity in the curve was clearly found under about 1 GPa. This observation clearly indicates that the phase transition of the pyrazine crystal takes place under pressure of about 1 GPa.

The characteristic behavior of the pressure–frequency

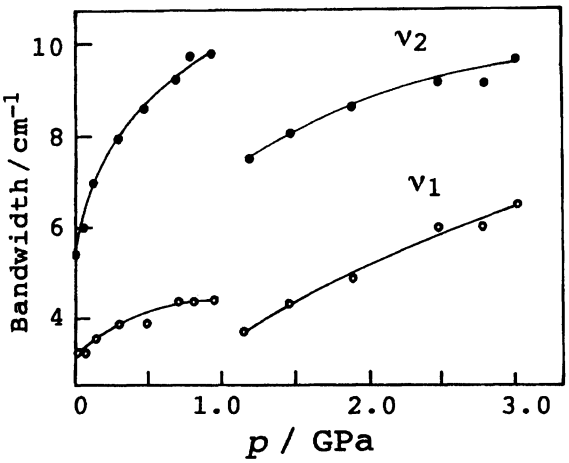

Fig. 5. Pressure effect on the bandwidths of the ν_2 (•–•–•) and ν_1 (o–o–o) vibrations observed at 297 K.

curve for the intermolecular vibrations, the discontinuity in the pressure-bandwidth curve for the intramolecular vibrations, and the calculated value of the pressure-induced frequency shift lead to the conclusion that the pyrazine crystal undergoes the phase transition (change of the molecular orientation in the crystal) under pressure about 1 GPa.

References

1) M. M. Thiéry and J. M. Léger, *J. Chem. Phys.*, **89**, 4255 (1988).

2) W. D. Ellenson and M. Nicol, *J. Chem. Phys.*, **61**, 1380 (1974).

3) D. M. Adams and R. Appleby, *Proc. R. Soc. London, Ser. A*, **296**, 1986 (1977).

4) F. Cansell, D. Fabre, and J. P. Petitet, *J. Chem. Phys.*, **99**, 7300 (1993).

5) S. Matsukuma, H. Kawano, Y. Nibu, H. Shimada, and R. Shimada, *Bull. Chem. Soc. Jpn.*, **67**, 1588 (1994).
6) G. Sadakuni, M. Maehara, H. Kawano, Y. Nibu, H. Shimada, and R. Shimada, *Bull. Chem. Soc. Jpn.*, **67**, 1593 (1994).
7) R. M. Hexer, *J. Chem. Phys.*, **33**, 1833 (1960)
8) D. A. Dows, *J. Chem. Phys.*, **32**, 1342 (1960).
9) F. D. Verderame, J. A. Lannon, L. E. Harris, W. G. Thomas, and E. A. Lucia, *J. Chem. Phys.*, **56**, 2638 (1972).
10) P. J. Miller, S. Block, and G. J. Piermarini, *J. Chem. Phys.*, **93**, 462 (1989).
11) H. Kawano, M. Maehara, Y. Nibu, H. Shimada, and R. Shimada, *Bull. Chem. Soc. Jpn.*, **67**, 2308 (1994).
12) R. Shimada, H. Kawano, Y. Nibu, H. Shimada, *Res. Bull. Fukuoka Institute of Technology*, **27**, 79 (1994).
13) J. D. Simmons, K. K. Innes, and G. M. Begun, *J. Mol. Spectrosc.*, **14**, 190 (1964).
14) S. Califano, G. Adembri, and G. Sbrana, *Spectrochim. Acta*, **20**, 385 (1964).
15) G. Sbrana, V. Schettino, and R. Righini, *J. Chem. Phys.*, **59**, 2441 (1973).
16) J. Zarembowitch and L. Bokobza-Sebagh, *Spectrochim. Acta, Part A*, **32A**, 605 (1976).
17) K. Matsuzaki, M. Sasaki, and T. Azumi, *J. Chem. Phys.*, **65**, 3326 (1976).
18) F. Kokai and T. Azumi, *J. Chem. Phys.*, **77**, 2757 (1982).
19) Y. Udagawa, M. Ito, and I. Suzuka, *Chem. Phys.*, **46**, 237 (1980).
20) D. McDonald and S. A. Rice, *J. Chem. Phys.*, **74**, 4893 (1981).
21) T. Hieida, M. Maehara, Y. Nibu, H. Shimada, and R. Shimada, *Bull. Chem. Soc. Jpn.*, **62**, 2989 (1989).
22) M. Ito and T. Shigeoka, *J. Chem. Phys.*, **44**, 1001 (1966).
23) B. Pasquier, D. Bougeard, N. le Calve, and R. Romain, *Mol. Cryst. Liq. Cryst.*, **32**, 17 (1976).
24) T. Hieida, M. Maehara, Y. Nibu, H. Shimada, and R. Shimada, *Bull. Chem. Soc. Jpn.*, **62**, 925 (1989).
25) V. Schettino, G. Sbrana, and R. Righini, *Chem. Phys. Lett.*, **13**, 284 (1972).
26) H. -H. Perkampus and E. Baumgarten, *Spectrochim. Acta*, **19**, 1473 (1963).
27) H. K. Mao, P. M. Bell, J. W. Shaner, and D. J. Steinberg, *J. Appl. Phys.*, **49**, 3276 (1978).
28) M. A. Spackman, *J. Chem. Phys.*, **85**, 6579 (1986).
29) H. Bonadeo and E. D'Alessio, *Chem. Phys. Lett.*, **19**, 117 (1973).
30) Y. Ishibashi, F. Arakawa, H. Shimada, and R. Shimada, *Bull. Chem. Soc. Jpn.*, **56**, 1327 (1983).
31) G. de With, S. Harkema, and D. Feil, *Acta Crystallogr., Sect. B*, **B32**, 3178 (1976).
32) S. N. Vaidya and G. C. Kennedy, *J. Chem. Phys.*, **55**, 987 (1971).
33) F. Cansell, D. Fabre, and J. P. Petitet, *J. Chem. Phys.*, **99**, 7300 (1993).